# Self-Assembly of Amphiphilic Block Copolymers: The $(EO)_{13}(PO)_{30}(EO)_{13}$−Water−*p*-Xylene System

**Paschalis Alexandridis,* Ulf Olsson, and Björn Lindman**

*Physical Chemistry 1, Chemical Center, University of Lund, Lund, S 22100, Sweden*

*Received May 24, 1995; Revised Manuscript Received August 15, 1995*[⊗]

ABSTRACT: The self-assembly of a poly(ethylene oxide)-*block*-poly(propylene oxide)-*block*-poly(ethylene oxide) copolymer (Pluronic L64, $(EO)_{13}(PO)_{30}(EO)_{13}$) in the presence of water and *p*-xylene was investigated. The phase boundaries were identified using $^2H$ NMR of heavy water ($^2H_2O$) and inspection under polarized light. Small-angle X-ray scattering was employed to ascertain the structure of the various liquid crystalline phases formed and to determine the structural lengths involved. A rich phase behavior with normal hexagonal, lamellar, bicontinuous cubic, and reverse hexagonal liquid crystalline regions, in addition to three separate liquid phases, was observed at 25 °C. The cubic phase was identified as having a structure associated with the Gyroid minimal surface. A very small liquid region, found between the normal hexagonal and lamellar phases on the binary water−polymer axis, is identified as a melted analogue of a bicontinuous cubic phase often present in this part of the phase diagram. The pure polymer exists at 25 °C as a disordered melt. Structure and segregation are induced by the addition of water. *p*-Xylene is soluble in the polymer melt but does not induce structure when added alone. For polymer concentrations above ~50%, a sequence of liquid crystalline phases is observed when the water-to-oil ratio is varied. Here we can identify the volume fraction of apolar components, given by the sum of the PPO and oil volume fractions, as the major parameter governing the phase behavior.

## INTRODUCTION

Poly(ethylene oxide)-*block*-poly(propylene oxide)-*block*-poly(ethylene oxide) (PEO−PPO−PEO) copolymers are nonionic macromolecular surface-active agents, available commercially as Poloxamer, Synperonic, or Pluronic polyols. Variation of the copolymer molecular weight and composition leads to compounds with hydrophilic−lipophilic properties that meet the specific requirements in different applications, such as detergency, dispersion stabilization, foaming, emulsification, and lubrication; their low toxicity makes them also suitable for pharmaceutical usage.[1,2]

A number of PEO−PPO−PEO copolymers have been shown to self-associate in water (at concentrations that depend strongly on the temperature[3,4]) in the form of micelles that have a core composed of PPO and a corona dominated by hydrated PEO segments (see refs 5 and 6 for recent reviews on the properties of the PEO−PPO−PEO copolymers in aqueous solutions). The formation of micelles and their shape and size have been investigated by a number of researchers using various techniques and are relatively well understood.[5,6] Some PEO−PPO−PEO copolymers have been known to form "gels" in water,[2,6,7] but the rich phase behavior of these copolymers in a binary system with water has only recently been recognized.[8−10] Depending on the copolymer molecular weight and composition, cubic, hexagonal, and/or lamellar mesophases can be formed at higher copolymer concentrations (>20%).[8−10] Some of the "gel" phases reported in the literature correspond to a cubic organization[5,6] while others still lack proper structural identification.

Although the PEO−PPO−PEO copolymers are good emulsifiers[1] and can solubilize hydrophobic compounds in aqueous micellar solutions,[11] the phase behavior of ternary copolymer−water−oil systems has received very little attention. Chu and co-workers[12−14] studied the water-induced micelle formation of a PEO−PPO−PEO copolymer (Pluronic L64) in *o*-xylene. Light,[12] small-angle X-ray,[13] and neutron[14] scattering were used to obtain information on the micelle size and structure. The existence of a lamellar structure at polymer concentrations of >0.53 g/mL has also been reported.[15] However, the composition range studied in refs 12−14 was rather limited. Moreover, the report on the lamellar structure[15] was ill-founded; as we show below, the structure corresponding to the compositions studied in ref 15 is hexagonal. In a sense, Chu et al. just scratched the surface of the rich phase behavior afforded by relatively short-chain amphiphilic block copolymers in water−oil mixtures.

We report here the first more complete phase diagram of a PEO−PPO−PEO copolymer (Pluronic L64)−water−oil ternary system, and we show that the copolymer molecules can self-assemble in a variety of structures depending on the composition. $^2H$ nuclear magnetic resonance (NMR) and small-angle X-ray scattering (SAXS) were the main techniques employed here to identify the boundaries and ascertain the structure of the various phases formed, respectively. The paper is organized as follows: After a description of the main features of the ternary L64−$^2H_2O$−*p*-xylene phase diagram, more details on each phase are presented. From the liquid crystalline phases, the lamellar is discussed first, being structurally more simple; the presentation of the normal and reverse hexagonal phases follows. The cubic phase, observed between the lamellar and reverse hexagonal regions, and the narrow liquid phase, present between the normal hexagonal and lamellar regions on the binary water−polymer axis, are analyzed next. The characteristic structural dimensions (obtained from SAXS) of the liquid crystalline phases are compared and discussed in terms of the configuration adopted by the polymer molecules. The phase behavior of the PEO−PPO−PEO block copolymer is related to that of "dry" block copolymers (polymer science point of view) and contrasted to that of alkyloligo(ethylene oxide) surfactants (surfactant science point of view). Finally, we consider the effect of the xylene isomer and report some results from the related L64−

* To whom correspondence should be addressed.

[⊗] Abstract published in *Advance ACS Abstracts,* October 1, 1995.

0024-9297/95/2228-7700$09.00/0 

water–*o*-xylene system, recently studied by others.[15] Our use of *p*-xylene rather than *o*-xylene was motivated by the simpler NMR properties of the former, due to the symmetric position of the two methyl groups, which we intend to utilize in future work.

## EXPERIMENTAL PROCEDURES

**Materials.** The Pluronic L64 poly(ethylene oxide)-*block*-poly(propylene oxide)-*block*-poly(ethylene oxide) copolymer was obtained as a gift from BASF Corp., Parsippany, NJ, and used as received. The copolymer has a nominal molecular weight of 2900 and ~40 wt % PEO (according to the manufacturer). This molecular weight and composition correspond to 26.3 ethylene oxide (EO) segments and 30.0 propylene oxide (PO) segments; thus L64 can be represented by the formula $(EO)_{13}$-$(PO)_{30}(EO)_{13}$. Wu et al.[12] obtained for this copolymer a number-average molecular weight ($M_n$) of 3400 g/mol using vapor pressure osmometry, and a weight-average molecular weight ($M_w$) of 3700 g/mol from static light scattering measurements, thus yielding $M_w/M_n = 1.1$, an indication of low polydispersity. $^2H_2O$ (99.80 atom % $^2H$) was purchased from Dr. Glaser AG, Basel, Switzerland, while *p*-xylene (1,4-dimethylbenzene) of >99.0% purity (as determined by GC) was obtained from Fluka Chemie AG, Buchs, Switzerland.

**Sample Preparation.** Samples were prepared individually by weighing appropriate amounts of polymer, water, and oil into 8 mm (i.d.) glass tubes which were flame-sealed immediately. The samples were centrifuged repeatedly in both directions over several days to facilitate mixing (when they were viscous) and then centrifuged in one direction to speed up phase separation (if not single phase). The samples were kept at a temperature-controlled room that was maintained at 25 ± 0.5 °C.

**Inspection under Polarized Light.** The texture of the liquid crystalline phases was examined between crossed polarizers and under an Axioplan Universal (Zeiss, Germany) polarizing microscope, equipped with a differential interference unit, a camera (MC100) for direct imaging, and a video system with image analysis facilities for automatic acquisition and examination. For normal surfactant systems, a lamellar liquid crystal displays a mosaic planar texture, while a hexagonal liquid crystal shows a fanlike angular or a striated nongeometric texture.[16] Cubic phases and isotropic liquids are recognized by not being optically birefringent.

**Water $^2$H-NMR Method.** The NMR spectrum of deuterated water is dominated by the interaction of the deuteron quadrupole moment with the electric field gradient tensor at the nucleus. For an anisotropic liquid crystalline sample, this quadrupole interaction generates a spectrum with two equally intense peaks. In an isotropic solution, on the other hand, this interaction is averaged to zero as a result of rapid and isotropic molecular motions, and the spectrum will consist of a singlet. An observed quadrupole splitting $\Delta(^2H)$ depends on the fraction of deuterons in one or more anisotropic sites, the quadrupole coupling constant, and the average molecular ordering of water molecules in the sites. A detailed theoretical treatment of $^2$H quadrupole splitting in lyotropic liquid crystalline phases can be found in ref 17. It has been shown that $^2$H NMR of deuterated water can be conveniently used to study the phase equilibria of amphiphile–water systems.[18]

For a heterogeneous system consisting of two or more phases, one expects a superposition of the $^2$H-NMR spectra representative of each phase, provided that the deuteron exchange between the phases is slow. Thus, for a system containing a mixture of a lamellar and a hexagonal liquid crystalline phase, two quadrupole splittings will be observed. The splitting from the hexagonal phase is generally smaller than the one from a lamellar phase of similar composition, since the quadrupolar coupling in the hexagonal phase is further averaged by diffusion around the cylinder axis.[17] For a three-phase system consisting of two anisotropic liquid crystalline phases and one isotropic phase, the $^2$H-NMR spectrum will contain two doublets and a central singlet, while for a two-phase system with one anisotropic and one isotropic phase, a doublet and a central singlet will be observed. However, the existence of two or more isotropic phases can normally not be established by the $^2$H-NMR method.

$^2$H-NMR experiments were performed at a resonance frequency of 15.371 MHz (2.3 T) on a Bruker MSL100 pulsed super-conducting spectrometer working in the Fourier transform mode. The sample temperature was maintained at 25 ± 0.5 °C during the NMR measurement by passing air of controlled temperature through the sample holder. The quadrupole splittings ($\Delta^2$H) were measured as the peak-to-peak distance and are given in frequency units (Hz).

**Small-Angle X-ray Scattering.** SAXS measurements were performed on a Kratky compact small-angle system equipped with a position sensitive detector (OED 50M, MBraun, Graz, Austria) containing 1024 channels of 51.3 μm width. Cu Kα radiation of wavelength 1.524 Å was provided by a Seifert ID-300 X-ray generator, operating at 50 kV and 40 mA. A 10 μm thick nickel filter was used to remove the Kβ radiation, and a 1.5 mm tungsten filter was used to protect the detector from the primary beam. The X-ray beam width (at half the maximum intensity) was 0.52 mm. This value is low and would lead to negligible smearing effects on the SAXS profiles over the $q$ range of interest; we thus used the peak positions of the smeared spectra in the analysis of the SAXS structural data presented here. The sample-to-detector distance was 277 mm. The sample stage K-PR allows temperature control in the range 0–70 °C, with an accuracy of 0.1 °C, by using a Peltier element. The volume between the sample and the detector was under vacuum during the measurements in order to minimize background scattering from air.

The samples (always single phase) used for SAXS measurements were filled into a quartz capillary using a syringe. This quartz capillary is glued to an invar steel body which is designed to make possible simultaneous small- and wide-angle measurements. The cuvette is stoppered using screw caps. The viscosity of the samples increased in the sequence lamellar < hexagonal < cubic, but it was still possible to inject the sample. The injection procedure may result in some orientation of the sample with respect to the capillary wall, but we expect this to work to our advantage (i.e., lead to sharper peaks) and not affect the structure type. In fact, we have checked on a number of occasions the capillary sample holder against one for pastelike or solid materials and observed no difference in the peak positions and relative intensity.

**Definitions of Polar and Apolar Domain Volume Fractions and Interfacial Area.** The L64 triblock copolymer molecule consists of a PPO middle block and two PEO end blocks. The PPO block is less polar than the PEO blocks[19] and thus aggregates are formed with domains that are rich in PPO (and oil) and domains that are rich in PEO (and water). The difference in polarity between the "hydrophilic" PEO blocks and the "hydrophobic" PPO block is smaller than, for example, the polarity difference between "head group" and (usually hydrocarbon) "tail" in normal surfactants. Consequently, in the ternary polymer–water–oil system, the PPO-rich domains may contain a certain amount of water and the PEO domains a certain amount of oil. Furthermore, the interface between the polar (PEO + water) and apolar (PPO + oil) domains is expected to be less sharp but with smooth and extended concentration profiles across the interface.[6,11,19] The concentration profiles in the ternary system is at present unknown.

To a first approximation, we may still ignore the partitioning of water and oil in the PPO and PEO domains, respectively, and consider the system as strongly segregated. We can then define an apolar volume fraction, $f$, containing oil and PPO and the remaining polar volume fraction, $(1 - f)$, containing water and PEO. From the bulk density values of PEO and PPO we estimated that the PPO block, which is the 60% of the polymer weight, makes up ~62% of the polymer volume. With this assumption, we define the apolar and polar volume fractions as

$$f = \Phi_o + 0.62\Phi_p$$

$$1 - f = \Phi_w + 0.38\Phi_p \quad (1)$$

where $\Phi_p$, $\Phi_o$, and $\Phi_w$ are the polymer, oil, and water volume

fractions, respectively. The bulk density of L64 (according to the manufacturer) is 1.05 g/mL at 25 °C, corresponding to a molecular volume of $\sim v_p = 4600$ Å$^3$ for a polymer of nominal molecular weight 2900. In our calculations we have used the (bulk) density values of 1.104 and 0.861 g/mL for heavy water ($^2H_2O$) and *p*-xylene, respectively. We also assumed that the partial molar volumes of the various components are independent of the composition. We note that the density of the polymer in solution and in the various aggregates may be different from the bulk value;[19] However, the polymer concentration in the samples of interest here is quite large (>50%), and thus the use of the bulk density appears justified.

The interfacial area that the block copolymer occupies is evaluated at the polar–apolar interface according to the definitions of those two domains above. The interfacial area per unit volume, $A/V$, can be expressed as

$$A/V = 2\Phi_p a_p / v_p \quad (2)$$

where $a_p$ is the interfacial area per PEO block (hence the total interfacial area per PEO–PPO–PEO triblock copolymer molecule is $2a_p$). The use of the L64 molecular weight values obtained by Wu et al.,[12] instead of the nominal 2900 value used here in the data analysis, would result in $v_p$ and $a_p$ values higher by 10–20% than the ones reported here.

Equation 2 assumes that all the polymer participates at the interface between water and oil. The unimer (unassociated polymer) concentration in aqueous L64 solutions is rather high (7% at 25 °C as interpolated from the data of ref 3), suggesting that the assumption of eq 2 may not be valid. The following experimental findings, however, support the use of eq 2: (i) The cmc of aqueous surfactant solutions, and of PEO–PPO–PEO copolymer solutions in particular, decreases in the presence of oils such as xylene.[20] (ii) The cmc of the PEO–PPO–PEO copolymers decreases dramatically with increasing temperature.[3] If the presence of unimers was affecting the lamellar structure, one would expect a big change in its characteristic dimensions between different temperatures; however, this was not observed[10] for Pluronic L64 in water.

**Determination of the Phase Diagram.** The samples were first examined by ocular inspection, against scattered light, and between crossed polaroids to check for sample homogeneity and birefringence. This provided a quick indication of the boundaries between isotropic and nonisotropic phases as well as between one- and two-phase regions. The ease with which the samples flowed was also used in the phase determination; micellar phases were fluid, lamellar phases were viscous but could flow (e.g., when the glass tube containing the sample was inverted), hexagonal phases flowed with more difficulty, and cubic phases were very stiff. The above procedures were repeated over a period of a few weeks to ensure that an equilibrium was reached. Adequate equilibration time was allowed before the study of the phase diagram; once established, the boundaries of the various phases in the phase diagram did not change over a period of 8 months.

From the general appearance of the $^2$H-NMR spectra it was established whether a certain sample consisted of a single homogeneous phase or was heterogeneous, i.e., composed of two or three phases. The presence of an isotropic phase is directly noted from a sharp singlet, and that of an anisotropic phase from a doublet of broad peaks (as discussed above). The identification of the hexagonal and lamellar liquid crystalline phases was achieved by starting with samples showing two doublets and the prediction of a larger quadrupole splitting for the lamellar phase than for the hexagonal phase.[21] The structure of the various liquid crystalline phases formed was confirmed by the reflections identified in SAXS spectra. It was thus possible from a systematic variation of composition, and using the techniques outlined above, to establish with good precision (better than ±1.25%) the entire phase diagram.

A practical problem in the study of the liquid crystalline phases in amphiphilic systems is that it sometimes may be extremely difficult to separate the individual phases from each other, especially if they have similar densities and/or are very viscous.[21] The determination of the phase diagram by following the $^2$H-NMR spectra of different samples is a nondestructive method which does not require a macroscopic separation of the individual phases of a mixture. For the present study, the $^2$H-NMR method was very suitable and led to a facile and rapid establishment of most features of the phase diagram.

**Normal vs Heavy Water.** Heavy water is slightly less polar than normal water (the dielectric constant of $^2H_2O$, 77.94 at 25 °C, is 0.76% lower than the one of $^1H_2O$, 78.54 at 25 °C) and is known to affect to a small extent the cmc of surfactants and of PEO–PPO–PEO copolymers in particular (see, for example, Figure 8 in ref 22). Since the environment afforded by $^2H_2O$ is not that different from the one afforded by $^1H_2O$, the substitution of $^1H_2O$ with $^2H_2O$ is not expected to change the features of the phase diagram that we present in this paper. The advantages of $^2H_2O$ in (i) the straightforward determination using $^2$H NMR of the composititon of two-phase samples and in (ii) facilitating phase separation (because of its higher density than $^1H_2O$) far outweigh the inconvenience of slight changes in the phase boundaries when one switches from $^2H_2O$ to $^1H_2O$.

## RESULTS AND DISCUSSION

**Overview of the Phase Behavior.** The isothermal phase diagram obtained at 25 °C for the ternary system $(EO)_{13}(PO)_{30}(EO)_{13}$ (Pluronic L64)–water–*p*-xylene is presented in Figure 1. It contains two isotropic solution phases, one rich in water ($L_1$) and one with a high *p*-xylene-to-water ratio ($L_2$), and four liquid crystalline phases, a normal hexagonal ($H_1$), a lamellar ($L_\alpha$), a cubic ($V_2$), and a reverse hexagonal ($H_2$). In addition to the above, a narrow isotropic phase (L′) is found between the $L_1$ and the $H_1$ regions. In the oil-lean part of the phase diagram (along the polymer–water binary axis), the amphiphilic copolymer self-assembles upon increase of its concentration into a micellar isotropic solution, a hexagonal liquid crystalline structure, a narrow liquid isotropic phase, a lamellar structure, and finally a polymer-rich isotropic phase. The sequence of hexagonal, lamellar, reverse hexagonal, and $L_2$ phases is observed by replacing water by oil at a constant polymer weight fraction of ~0.5. A description of the different phases and their respective structures is given in the ensuing sections.

The two-phase regions $L_1$–$L_\alpha$, $L_1$–$H_1$, $H_1$–$L_\alpha$, $H_1$–L′, L′–$L_\alpha$, $L_\alpha$–$L_2$, $L_\alpha$–$H_2$, $L_\alpha$–$V_2$, $V_2$–$H_2$, and $H_2$–$L_2$, as well as the three-phase triangles $L_1$–$H_1$–$L_\alpha$, $L_1$–$L_\alpha$–$L_2$, $L_\alpha$–$H_2$–$L_2$, $H_1$–L′–$L_\alpha$, $L_\alpha$–$V_2$–$H_2$, and $L_\alpha$–$H_2$–$L_2$, are also shown in Figure 1. The boundaries of the multiphase regions were drawn based on optical inspection and $^2$H quadrupolar splitting values. The boundaries of the $L_1$–$H_1$–$L_\alpha$, $L_1$–$L_\alpha$–$L_2$, and $L_\alpha$–$H_2$–$L_2$ triangles are tentative. Accurate determination of the boundaries was hindered by the formation of stable (i.e., no macroscopic phase separation over a period of 8 months) emulsions especially at low (<20%) polymer content. The three-phase $L_1$–$L_\alpha$–$L_2$ region dominates the low-polymer-content part of the phase diagram. The stable emulsions observed in this region could be attributed to the presence of lamellae ($L_\alpha$) which coat (and thus stabilize) the water or oil microdroplets. Stable emulsions are known to occur in $L_1$–$L_\alpha$–$L_2$ three-phase regions formed by ordinary surfactants.[23]

**Isotropic Water-Rich ($L_1$) and Oil-Rich (Water-Lean) ($L_2$) Regions.** The L64 PEO–PPO–PEO copolymer dissolves in heavy water at 25 °C and forms an isotropic solution phase up to ~46% by weight of polymer. The L64 molecules are dissolved in water as individual polymer chains (unimers) up to polymer concentrations of 7 wt % (at 25 °C).[3] At higher concentrations the copolymer molecules self-assemble into

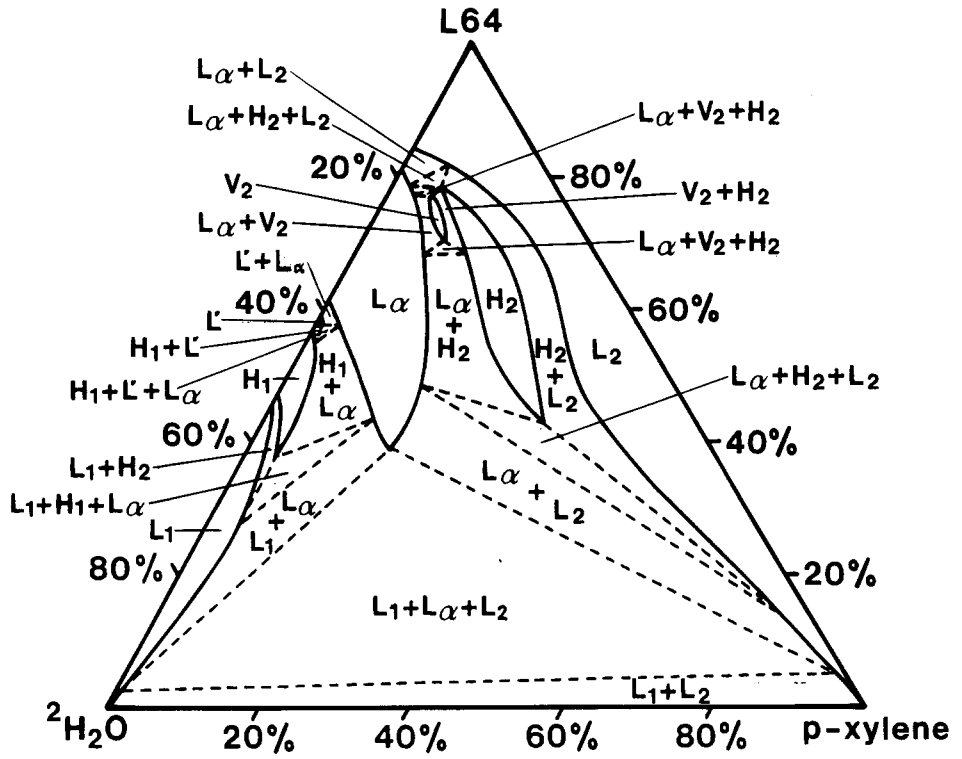


**Figure 1.** Phase diagram of the $(EO)_{13}(PO)_{30}(EO)_{13}$ (Pluronic L64)–water–*p*-xylene ternary system at 25 °C. The phase boundaries of the one-phase regions are drawn with solid lines, while the boundaries of the two-phase regions and the three-phase triangles are indicated with dotted lines. The concentrations are expressed in weight percent. $L_1$, L′, $H_1$, $L_\alpha$, $V_2$, $H_2$, and $L_2$ denote water-rich (normal micellar) solution, bicontinuous liquid, normal hexagonal, lamellar, reverse bicontinuous cubic, reverse hexagonal, and oil-rich (reverse micellar) phases, respectively.

spherical micelles with a hydrophobic core consisting mainly of PO segments and a corona composed of highly hydrated EO segments (there are about 10–20 water molecules per EO segment in the corona region).[5,6] The aggregation number and hydrodynamic radius of the micelles have been investigated as a function of temperature by a number of researchers (see refs 5 and 6 and references cited therein). The aqueous solutions have the capability of solubilizing *p*-xylene at most up to ~4% by weight. The xylene uptake by the PEO–PPO–PEO micelles is rather low compared to that of alkyloligo(ethylene oxide) surfactants, reflecting the inability of the L64 micelles to swell.

Pluronic L64 is miscible with *p*-xylene in all proportions, and the $L_2$ phase extends along the whole water-lean side of the phase diagram. L64 does not form polymolecular micelles in *o*-xylene in the absence of water or even when a small amount of water (up to ~0.15 water molecules/EO segment) is present.[12] Micelles with a hydrated PEO core and a PPO corona are apparently formed by L64 in *p*-xylene at higher water concentrations. It was found[14] from SANS experiments in the L64–water–*o*-xylene system that the solubilized water existed not only in the micelle core but also in the shell. However, the volume fraction of water in the micelle shell was much smaller than that in the core.[14] We note that the maximum amount of water taken up by the micelles is ~1/3 of the polymer weight, as evidenced by the phase boundary between the $L_2$ and the two-phase region. This indicates that ~2 water molecules/EO segment can be solubilized in *p*-xylene. This relationship holds up to ~50% polymer; it is likely that at high polymer concentrations the micelle structure becomes less well defined and both water and xylene are dissolved in the polymer. A total of 12 wt % water can be incorporated in the polymer–oil solution.

It is interesting to compare the PEO–PPO–PEO copolymer solution behavior in oil ($L_2$ phase) with the behavior of the so-called associative thickeners in water, where they are commonly used for modifying the rheological properties. Associative thickeners are typically triblock copolymers having water-soluble middle block (typically PEO) and water-insoluble end blocks (typically alkyl chains).[24] In aqueous solutions, the hydrophobic end blocks of associative thickeners self-assemble into aggregates where the middle block acts as a cross-linker when the two end block participate in different aggregates. This results in a very high viscosity of the solutions, attained often already at low concentrations of the associative thickener. The Pluronic PEO–PPO–PEO molecule has the same type of architecture except that here the middle block is the more hydrophobic. Hence, one might expect a similarly high viscosity in the $L_2$ phase if the PEO blocks would associate into aggregates with the possibility for the PPO block to cross-link. However, the viscosity of the $L_2$ phase is everywhere relatively low, with no signs of cross-link effects. This is consistent with no or only weak aggregation in the $L_2$, which is supported by the fact that the $L_2$ phase extends over the whole polymer concentration range. In a case of significant aggregation we would expect the formation of liquid crystalline mesophases at higher polymer concentrations as is observed along the L64–water binary axis; this is not the case with the binary L64–*p*-xylene system.

**Lamellar Phase ($L_\alpha$).** A lamellar phase is formed on the binary water–L64 axis at copolymer concentrations greater than 61% and continues up to ~81% per weight polymer. The lamellar phase extends well into the phase diagram and can accommodate up to 20 wt % *p*-xylene, suggesting swelling of the lamellae by *p*-xylene (contrary to what was observed in the $L_1$ and

**Table 1. Results from SAXS Experiments Performed on Various Compositions in the L64–Water–*p*-Xylene System**

| weight fraction | | | volume fraction | | | | | | | | |
|---|---|---|---|---|---|---|---|---|---|---|---|
| L64 | water | oil | L64 | water | oil | $f^a$ | phase[b] | $d$,[c] $a^c$/Å | $\delta^d$/Å | $R_{cyl}^e$/Å | $a_p^f$/Å$^2$ |
| 0.800 | 0.200 | 0 | 0.808 | 0.192 | 0 | 0.501 | $L_\alpha$ | 71 | 35 | | 80 |
| 0.700 | 0.300 | 0 | 0.711 | 0.289 | 0 | 0.441 | $L_\alpha$ | 75 | 33 | | 87 |
| 0.700 | 0.250 | 0.050 | 0.701 | 0.238 | 0.061 | 0.496 | $L_\alpha$ | 75 | 37 | | 87 |
| 0.550 | 0.300 | 0.150 | 0.540 | 0.280 | 0.180 | 0.515 | $L_\alpha$ | 93 | 48 | | 92 |
| 0.450 | 0.400 | 0.150 | 0.444 | 0.375 | 0.181 | 0.456 | $L_\alpha$ | 110 | 50 | | 94 |
| 0.550 | 0.450 | 0 | 0.562 | 0.438 | 0 | 0.384 | $H_1$ | 91 | | 28 | 101 |
| 0.475 | 0.525 | 0 | 0.488 | 0.512 | 0 | 0.303 | $H_1$ | 92 | | 27 | 107 |
| 0.700 | 0.150 | 0.150 | 0.683 | 0.139 | 0.178 | 0.601 | $H_2$ | 92 | | 30 | 88 |
| 0.550 | 0.200 | 0.250 | 0.526 | 0.182 | 0.292 | 0.618 | $H_2$ | 111 | | 36 | 92 |
| 0.450 | 0.200 | 0.350 | 0.422 | 0.178 | 0.400 | 0.662 | $H_2$ | 135 | | 41 | 89 |
| 0.700 | 0.200 | 0.100 | 0.692 | 0.188 | 0.120 | 0.549 | $V_2$ | 202 | 38 | | 87 |

[a] Total volume fraction of apolar material, defined according to eq 1. [b] $H_1$ denotes normal hexagonal phase, $L_\alpha$ denotes lamellar phase, $V_2$ denotes bicontinuous cubic phase, and $H_2$ denotes inverse hexagonal phase. [c] Lattice parameter. In the $L_\alpha$ phase we report the smectic repeat distance, $d$. In the $H_1$ and $H_2$ phases we report the lattice parameter, defined in eq 5. In the $V_2$ phase we report the lattice parameter $a = 2\pi 6^{1/2}/q_{211}$, where $q_{211}$ is the position of the first peak in the SAXS spectrum which is assigned to $hkl = 211$. [d] Apolar lamellar thickness in the lamellar and bicontinuous cubic phases. [e] Cylinder radius. In the normal hexagonal phase this is the radius of the apolar core cylinder, while in the reverse hexagonal phase it is the radius of the polar core cylinder. [f] Area per PEO block. Since each L64 PEO–PPO–PEO molecule contains two PEO blocks, the area per copolymer molecule is $2a_p$.

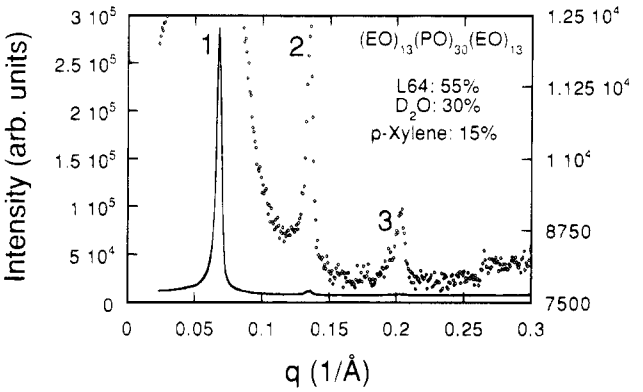


**Figure 2.** Slit-smeared SAXS spectrum obtained from the lamellar $L_\alpha$ liquid crystalline phase at a polymer–water–oil weight composition of 55.0:30.0:15.0 at 25 °C. The scattering curve is also shown on an expanded intensity scale (right-hand side) to reveal the higher order 2 and 3 Bragg peaks.

$H_1$ phases). The samples in this region are transparent, birefringent, and can flow under their own weight. They exhibit a splitting in the $^2$H-NMR spectrum with a higher value than the splitting in the $H_1$ phase. The one-dimensional lamellar structure was established by SAXS experiments that revealed sharp reflections obeying the 1:2 (and sometimes 1:2:3) relationship (see Table 1 and Figure 2).

A slit-smeared SAXS spectrum obtained from the lamellar liquid crystalline phase at a polymer–water–oil weight composition of 55.0:30.0:15.0 is presented in Figure 2 (plotted as a function of the scattering vector $q$). A second- and even a third-order peak can be observed and the 1:2:3 pattern confirms the lamellar structure.[25] The periodicity, $d$, of a lamellar structure is given by the lamellar area per unit volume ($A/V$). The position of the first order quasi Bragg peak, $q_1$, corresponds to

$$q_1 = 2\pi\Phi_p a_p / v_p \qquad (3)$$

Assuming a sharp interface, we may also calculate a thickness, $\delta$, of the apolar domain of the lamellae according to

$$d = \delta / f \qquad (4)$$

The corresponding thickness of the polar domains is then given by $d - \delta$.

$d$ spacings and $a_p$ and $\delta$ values obtained from various compositions in the lamellar phase are presented in Table 1. The $d$ values decreased with increasing polymer concentration at constant oil concentration (compare the samples with polymer–water–oil composition ratios 70.0:30.0:0 and 45.0:40.0:15.0 to the ones with compositions 80.0:20.0:0 and 55.0:30.0:15.0, respectively) and at constant water concentration (compare the samples with composition ratios 70.0:30.0:0 and 55.0:30.0:15.0). As the polymer concentration increases the amount of surface increases; thus the distance between the bilayers ($\sim d$) decreases. The area per PEO block is ~90 Å$^2$ but decreases slightly with increasing polymer concentration at both constant oil concentration and constant water concentration. Consequently, the apolar film thickness, $\delta$, increases with increasing polymer concentration, but it also increases with increasing oil content. The $\delta$ values are in the range 30–50 Å. The polar layer thicknesses ($d - \delta$) vary to a similar extent in the range 30–60 Å.

**Normal Hexagonal phase ($H_1$).** On the binary water–L64 axis, a normal hexagonal phase (denoted $H_1$) supersedes the micellar phase ($L_1$) at copolymer concentrations greater than 47% and extends up to ~57% per weight polymer (see Figure 1). Similarly to the $L_1$ phase, the hexagonal phase can solubilize only small amounts of *p*-xylene. The samples in this region are relatively stiff, transparent, and birefringent. They exhibit a splitting in the $^2$H-NMR spectrum, and the value of the splitting, $\Delta(^2H)$, increases by ~10% with increasing polymer concentration. The $\Delta(^2H)$ values in the $H_1$ phase were approximately half of the corresponding values in the $L_\alpha$ phase when the latter were extrapolated to the same water content as $H_1$; such a relationship is consistent with the cylindrical symmetry of the hexagonal phase.[17] The two-dimensional hexagonal structure was further established by SAXS experiments that revealed sharp reflections obeying the ratio $1:3^{1/2}:2$, characteristic of this structure.[25]

Figure 3 shows the slit-smeared SAXS spectrum that was obtained for a sample with a polymer–water–oil weight composition of 47.5:52.5:0. Three peaks can be resolved, corresponding to the relative positions $1:3^{1/2}:2$. By assuming a hexagonal structure, we can calculate the effective copolymer interfacial area and molecular length and compare these values with the ones obtained in the lamellar phase. For a two-dimensional hexagonal symmetry the diffraction peaks at $q_{hk}$, where $(h,k)$ are

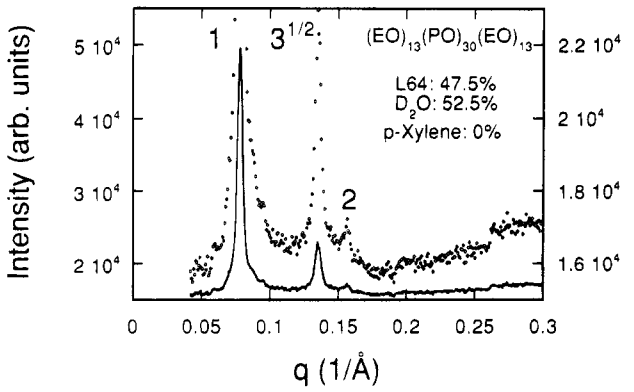


**Figure 3.** Slit-smeared SAXS spectrum obtained from the normal hexagonal $H_1$ liquid crystalline phase at a polymer–water–oil weight composition of 47.5:52.5:0 at 25 °C. The scattering curve is also shown on an expanded intensity scale (right-hand side) to reveal the higher order $3^{1/2}$ and 2 Bragg peaks.

the Miller indices, correspond to[26]

$$q_{hk} = (4\pi\sqrt{h^2 + k^2 + hk})/a\sqrt{3} \qquad (5)$$

where $a$ is the lattice parameter (nearest-neighbor distance). In the case of infinite cylinders of cross section radius $R_{cyl}$ and volume fraction $\Phi_{cyl}$ we have the relation[26]

$$R_{cyl} = a((\sqrt{3}/2\pi)\Phi_{cyl})^{1/2} \qquad (6)$$

Assuming a normal hexagonal structure and associating the apolar domains (i.e., *p*-xylene and the PPO blocks) with the interior of the cylinders ($f = \Phi_{cyl}$), we have

$$R_{cyl} = fv_p/a_p\Phi_p \qquad (7)$$

This corresponds to defining the polar–apolar interface at the interface separating the poly(ethylene oxide) and poly(propylene oxide) blocks of the copolymer. Equation 7 is derived from identifying $2a_p\Phi_p/v_p$ as the interfacial area per unit volume. Note, that the sequence of the three blocks in the L64 molecule is such that the PPO block will be in the interior of the cylinder, while both PEO blocks will be at the exterior. Substituting eqs 6 and 7 into eq 5 we then obtain

$$q_{hk} = \left(\frac{h^2 + k^2 + hk}{(\sqrt{3}/2\pi)f}\right)^{1/2} \frac{2a_p\Phi_p}{v_p} \qquad (8)$$

Values of the lattice parameter, $a$, the apolar cylinder radius, $R_{cyl}$, and the area per PEO block, $a_p$, are presented in Table 1 for two samples in the hexagonal phase. The area is slightly larger than in the lamellar phase, in the range 100–110 Å$^2$. The apolar cylinder radius is ~30 Å, and the lattice parameter is on the order of 90 Å.

**Reverse Hexagonal Phase ($H_2$).** A fairly extensive reverse hexagonal phase ($H_2$) is formed between the $L_\alpha$ and $L_2$ phases. $H_2$ is stable at copolymer concentrations greater than 43% and extends up to ~78% per weight polymer; the water concentration varies between 13 and 22 wt %. The samples in this region are transparent, birefringent, and rather stiff. The two-dimensional hexagonal structure was confirmed by SAXS experiments that revealed sharp reflections obeying the relationship $1:3^{1/2}:2$ (and sometimes $1:3^{1/2}:2:7^{1/2}$ as shown, e.g., in Figure 4).

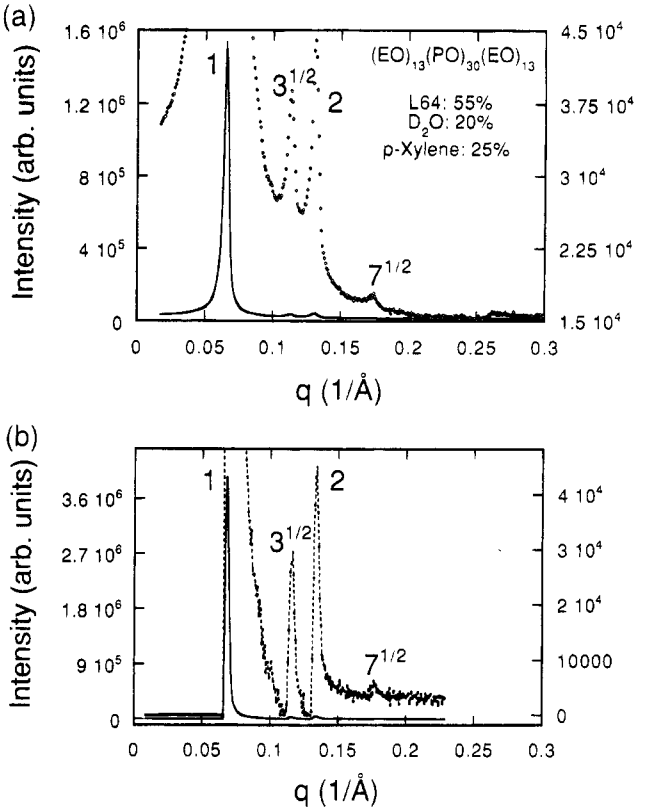


**Figure 4.** (a) Slit smeared and (b) -desmeared SAXS spectra obtained from the reverse hexagonal $H_2$ liquid crystalline phase at a polymer–water–oil weight composition of 55.0:20.0:25.0 at 25 °C (the desmearing was done according to the direct method of beam-height correction introduced by Singh, M. A.; Ghosh, S. S.; Shannon, R. F., Jr. *J. Appl. Cryst.* **1993**, *26*, 787). The scattering curves in both (a) and (b) are also shown on an expanded intensity scale (right-hand side) to reveal the higher order $3^{1/2}$, 2, and $7^{1/2}$ Bragg peaks.

Figure 4a shows a slit-smeared SAXS spectrum obtained for the reverse hexagonal liquid crystalline phase at a polymer–water–oil weight composition of 55.0:20.0:25.0 at 25 °C. The scattering curve is also shown on an expanded intensity scale (right-hand side) to reveal the higher order $3^{1/2}$, 2, and $7^{1/2}$ Bragg peaks. The desmeared SAXS data are shown in Figure 4b; it can be seen that desmearing has a very small effect on the information obtained by the SAXS spectra. By assuming a reverse hexagonal structure, we can calculate the effective copolymer area and cylinder radius values from the SAXS repeat distance in a manner similar to that of the normal hexagonal structure (see above). In analogy with eqs 6–8, we have for the reverse hexagonal phase

$$R_{cyl} = a\left(\frac{\sqrt{3}}{2\pi}(1 - f)\right)^{1/2} = \frac{(1 - f)v_p}{a_p\Phi_p} \qquad (9)$$

and

$$q_{hk} = \left(\frac{h^2 + k^2 + hk}{(\sqrt{3}/2\pi)(1 - f)}\right)^{1/2} \frac{2a_p\Phi_p}{v_p} \qquad (10)$$

In Table 1 we present values of $a$, $R_{cyl}$, and $a_p$ for three different samples within the reverse hexagonal phase area. $a_p$ is found to be relatively constant, ~90 Å$^2$, within the phase. The cylinder radius increases with increasing water-to-polymer ratio with values in the

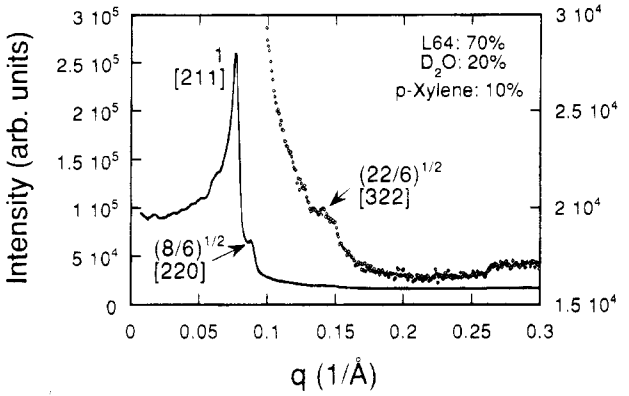


**Figure 5.** Slit-smeared SAXS spectrum obtained from the reverse cubic $V_2$ liquid crystalline phase at a polymer–water–oil weight composition of 70.0:20.0:10.0 at 25 °C. The scattering curve is also shown on an expanded intensity scale (right-hand side) to reveal the higher order $(8/6)^{1/2}$ and $(22/6)^{1/2}$ Bragg peaks.

range 30–40 Å. The lattice parameter varies within the range 90–140 Å.

**Bicontinuous Cubic Phase ($V_2$).** A small region of a cubic phase, denoted $V_2$, is formed between the $L_\alpha$ and $H_2$ phases at high (~70%) polymer concentration. The homogeneous samples from this region are optically isotropic and very stiff. A SAXS spectrum obtained from a sample with a polymer–water–oil weight composition of 70.0:20.0:10.0 is shown in Figure 5. The scattering function is dominated by a strong correlation peak at $q$ = 0.076 Å$^{-1}$. A weaker reflection is observed at $q$ = 0.088 Å, and in addition, a broad hump is observed around $q$ = 0.15 Å$^{-1}$.

Scattering data from lyotropic cubic phases generally contain only a small number of reflections, which makes a proper indexation and space group determination essentially impossible. As is seen in Figure 5, the present system is no exception in this respect. The relative position of this cubic phase in the phase diagram (between the $L_\alpha$ and $H_2$ phases) indicates that its structure is bicontinuous with the curvature of the polar–apolar interface toward water.[27] In surfactant systems, bicontinuous cubic phases are often described in terms of a multiply connected bilayer separating two distinguishable and continuous domains of the same solvent.[28,29] The global arrangement of the bilayer can be consistently described in terms of minimal surfaces of cubic symmetry. With the present triblock copolymer, a monolayer film where the two PEO blocks are located on opposite side cannot be distinguished from a bilayer film where the two PEO blocks are located on the same side. However, from the expected curvature of the polar–apolar interface, we anticipate the block copolymer molecular arrangement to be such that an apolar film containing the PPO block and the oil forms a dividing surface between two polar domains containing the PEO blocks and water.

With surfactants, most bicontinuous cubic phases that show a sufficient number of reflections are found to be consistent with the crystallographic space group $Ia3d$ ($Q^{230}$) and the Gyroid minimal surface structure.[27] The two first reflections from this structure correspond to the 211 and 220 reciprocal planes and hence to the relative positions $6^{1/2}$ and $8^{1/2}$, respectively, with the 211 being the dominating reflection.[30,31] The relative positions and intensities of the two observed reflections in Figure 5 (at 0.076 and 0.088 Å$^{-1}$, respectively) are indeed consistent with this sequence, indicating that the present cubic phase is also of the Gyroid minimal surface structure. In some cases, structures corresponding to the so-called D (space group $Pm3n$, $Q^{223}$) and P (space group $Im3m$, $Q^{229}$) minimal surfaces have been reported.[27] The first two reflections from these two structures come as $2^{1/2}$, $3^{1/2}$ ($Pm3n$) and $2^{1/2}$, $4^{1/2}$ ($Im3m$), respectively, which are inconsistent with the data of Figure 5.

This identification of the Gyroid structure receives further support when we consider the area of the polar–apolar interface. The polar–apolar interfaces in the cubic phase can be described as two surfaces displayed on opposite sides of a minimal surface, each by a distance $L$.[29,32] The total interfacial area per unit volume ($A/V$) is given by

$$\frac{A}{V} = \frac{2\varsigma}{a}\left(1 + \frac{2\pi\chi^{u}}{\varsigma}\left(\frac{L}{a}\right)^{2}\right) \qquad (11)$$

where $a$ is the lattice parameter, $\varsigma$ is a dimensionless area constant, and $\chi^u$ is the Euler characteristic per unit cell of the minimal surface.[33] A similar relationship holds for the volume fraction enclosed between the two interfaces. We identify this volume fraction with $f$ and write

$$f = \frac{2\varsigma L}{a}\left(1 + \frac{2\pi\chi^{u}}{3\varsigma}\left(\frac{L}{a}\right)^{2}\right) \qquad (12)$$

Equation 12 may be solved for $L$, and with the identity $A/V = 2\Phi_p a_p/v_p$ (eq 2), we can then calculate $a_p$. For the Gyroid surface $\chi^u = -8$ and $\varsigma = 3.091$.[33] With these values, we obtain with eqs 11 and 12 $a_p$ = 87 Å$^2$, which is the same value as in the $L_\alpha$ and $H_2$ phases on each side of the $V_2$ phase. On the basis of both the consistency of the area per PEO block value and the relative positions and intensities of the two X-ray reflections, we conclude that the cubic phase structure identified here corresponds to the Gyroid structure, similarly to the majority of the surfactant bicontinuous cubic phases.

From an applications point of view, the bicontinuous cubic phase, which we identified in the ternary polymer–water–oil system, holds promise for the synthesis of novel nanoporous materials (organic analogues of zeolites) having highly ordered structure and controlled pore size. This can be achieved by either the polymerization (cross-linking) of the copolymers or the polymerization of reactive water-soluble or oil-soluble monomers which will participate in the "water" or "oil" component, respectively, of the ternary system. The preparation of a macroporous hydrogel by the polymerization of a hydrophilic monomer in a cubic phase stabilized by didodecyldimethylammonium bromide has been reported by Anderson and Ström.[34]

**Isotropic Liquid Phase (L′).** A very narrow (stable at ~58–59 wt % polymer) isotropic liquid phase is formed between the hexagonal and the lamellar phases. The existence of this narrow phase area was recently reported by Zhang and Khan.[9] Although they were not able to isolate a single-phase sample, they stipulated that it is a bicontinuous cubic phase. However, more recent work[10] by Khan and co-workers has corroborated our finding that the L′ phase is indeed liquid.

We expect the topology of the L′ phase to be bicontinuous since such a structure can attain a mean curvature of the polar–apolar interface that is intermediate between that of the hexagonal and the lamellar phases.[29] Bicontinuous cubic phases often occur be-

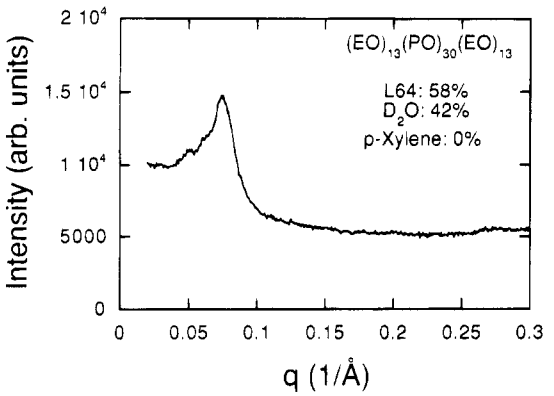


**Figure 6.** Slit-smeared SAXS spectrum obtained from the "melted cubic" L′ isotropic liquid phase at a polymer–water–oil weight composition of 58.0:42.0:0.0 at 25 °C.

tween the hexagonal and lamellar phases.[27] However, the L′ samples that we were able to isolate were of rather low viscosity; this is not consistent with a cubic arrangement, which normally has a very high viscosity. Furthermore, a SAXS spectrum, presented in Figure 6, shows a single broad correlation peak signifying a liquid phase with only short-range order. The fact that the phase is liquid and forms at the location where normally a bicontinuous cubic phase appears indicates that L′ can be considered as a disordered or melted version of the bicontinuous cubic phase, or a phase which often is referred to as the $L_3$ or "sponge" phase.[29]

**Interfacial Area per Polymer Molecule.** Based on the definition of polar and apolar domains (see the Experimental Procedures section) used here, we have determined from SAXS data the area per PEO block, $a_p$, in the various liquid crystalline phases formed in the L64–water–*p*-xylene system. The area value is ~90 Å$^2$ and varies slightly with the composition and phase structure. In the normal hexagonal phase we find a slightly larger PEO block area, namely, 100–110 Å. In the lamellar, bicontinuous cubic, and reverse hexagonal phases, however, the area remains fairly constant, ~90 Å$^2$, except at the higher polymer concentration in the lamellar phase where the area value drops to ~80 Å$^2$.

The above area per molecule values can be contrasted to the ones at the air–water interface as obtained from surface tension measurements.[35] The latter area per molecule values are approximately half the values in the liquid crystalline phases. The relatively small $a_p$ at the air–water interface was attributed to desorption of EO segments from the air–water interface and/or tightly packed segments.[35] The scaling of $a_p$ with the number, $N_{EO}$, of EO segments ($a_p \sim N_{EO}^{1/2}$) at the air–water interfacial layer intimated that the environment seen by the copolymer chains resembled that in polymer melt near an impenetrable wall.[35] The copolymer in the liquid crystalline phases may experience different conditions because of the swelling of both the PEO and PPO blocks by water and oil, respectively. Thus, the effective area per molecule at the oil/water interface is larger.

**Polymer Configuration.** An interesting question regarding the structures formed by the triblock copolymer concerns the relative position of the two end blocks in the aggregates. The architecture of the PEO–PPO–PEO polymer resembles that of the so-called "bolaform" or "bifunctional" surfactants.[36] NMR relaxation experiments performed on small spherical micelles formed by the bolaform surfactant *N*,*N*′-1,20-eicosanediylbis(triethylammonium bromide) showed that the preferred chain configuration was that with a large separation between the two head groups, i.e., a stretched conformation.[36] A preferred stretched conformation was also found when bolaform surfactants were introduced as guest molecules in a lipid bilayer. Unless the bilayer thickness was larger than the stretched length of the bolaform surfactant, a stretched conformation of the bolaform surfactant was found where the bolaform molecule spanned the bilayer with the two head groups on opposite sides.[37] Such behavior, which seems to be characteristic for the bolaform surfactants, is not expected with the PEO–PPO–PEO copolymer studied here.

Typical surfactants are characterized by a very strong segregation between the polar and apolar domains. Surfactant molecules pack more densely at the polar–apolar interface, and this reduces the number of possible chain conformations and induces a rather long effective persistence length of the hydrocarbon chain which can be of the order of the aggregate dimension. This can be seen from the order–parameter profile and from the fact that the radii of spherical surfactant micelles are approximately equal to the stretched hydrocarbon chain length. In the present triblock copolymer system, we expect the situation to be different. The packing at the interface is less dense, and the effective persistence length of the PPO is expected to be much smaller than the dimension of the PPO domain, which, in turn, is much smaller than the stretched PPO length. Consequently, we expect essentially no correlation between the location of the two PEO blocks in the aggregates. For example, in the lamellar phase we expect the probability of finding the two PEO blocks on the same side of the lamellae to be the same (50%) as that of finding them on opposite sides. Similarly, we expect no angular correlation between the locations of the PEO blocks in the normal cylindrical or spherical micelles. In the reverse hexagonal phase, where the interior of the cylinders contains water and the PEO blocks, the polymer has the possibility to form bridges between neighboring cylinders.

A schematic view of the possible configurations attained by the PEO–PPO–PEO copolymer molecules in the normal hexagonal, lamellar, and reverse hexagonal liquid crystalline phases is shown in Figure 7. A cross section perpendicular to the cylinder axis is shown for the normal and reverse hexagonal structures, while a cross section perpendicular to the bilayer plane is shown for the lamellar structure. The characteristic dimensions, obtained from SAXS, are also indicated in Figure 7. Polymer chains from adjacent aggregates (cylinders or bilayers) are in proximity and are expected to interact with each other. The stretched length for a L64 molecule can be estimated by considering the possible conformations for the PEO chain: zigzag, helix, and meander.[15] The stretched length of one PEO block is about 48, 36, and 27 Å for the zigzag, helix, and meander conformations, respectively. The stretched length of the PPO block is approximately twice that of PEO.

**Further Considerations on the Phase Behavior.** Phase diagrams of multicomponent mixtures containing amhiphiles are of technical and theoretical interest, and thus it is important to have a general understanding of the factors influencing various features of a phase diagram. A theoretical analysis of the observed phase equilibria is outside the scope of the present treatment, but a few qualitative remarks will be made.

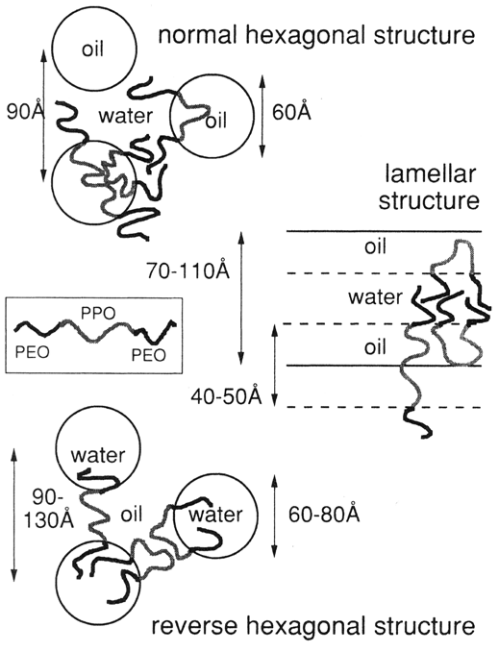


**Figure 7.** Schematic view of the possible configurations attained by the PEO–PPO–PEO copolymer molecules in the normal hexagonal, lamellar, and reverse hexagonal liquid crystalline phases. A cross section perpendicular to the cylinder axis is shown for the normal and reverse hexagonal structures, while a cross section perpendicular to the bilayer plane is shown for the lamellar structure. The characteristic dimensions, obtained from SAXS, are also indicated. The stretched length of a $(EO)_{13}(PO)_{30}(EO)_{13}$ molecule is ~120 Å.

A transition from normal micellar to normal hexagonal, lamellar, reverse hexagonal, and reverse micellar (with various cubic "intermediate" phases possible) is generally observed in surfactant systems upon increase in the surfactant concentration.[27] With reference to topology, there is a "mirror plane" through the lamellar liquid crystalline phase; phases on the water-rich side are considered to be of the "oil-in-water" type, while those on the water-poor side are considered to be of the "water-in-oil" type. The above formalism can be extended to cover the change in the curvature of the microstructures formed by the copolymer as the ratio of water to oil decreases. The sequence of normal hexagonal, lamellar, reverse hexagonal, and $L_2$ phases is indeed observed by replacing water by oil at a constant polymer weight fraction of ~0.5, whereas a reverse bicontinuous cubic phase is formed between the lamellar and the reverse hexagonal regions at a polymer weight fraction of ~0.75.

In addition to discussing the phase behavior of L64 in relation to that of short-chain amphiphiles, it is instructive to place the self-assembly of L64 in the context of the self-assembly of dry block copolymer systems.[38] Upon increase of the segregation ($\sim\chi N$, where $\chi$ is the Flory–Huggins segment–segment interaction parameter and $N$ is the number of segments) between the A and B blocks in a A–B diblock copolymer melt, an order–disorder transition occurs. In the limit $\chi N \gg 10$ ordered microstructures are formed with a topology (e.g., lamellar, cylindrical) that depends on the A–B composition of the block copolymer.[38] In the case of the L64–water–xylene system, the pure polymer can be considered as a disordered melt, whereupon structure and segregation are induced by the addition of water; *p*-xylene is soluble in the polymer melt but does not induce structure when added alone. For L64 concentrations above ~50%, a sequence of liquid crystalline phases is observed when the water-to-oil ratio is varied, similarly to the structure variation observed[38] in A–B block copolymer systems upon changing the A–B composition. Hence, we can identify the volume fraction of apolar components $f$, given by the sum of the PPO and oil volume fractions, as the major parameter governing the phase behavior. However, additional investigation of the self-assembly of PEO–PPO block copolymers in ternary systems of water and oil is needed to further establish the attributes governing the phase behavior.

**Comparison of PEO–PPO–PEO Block Copolymer Phase Behavior To That of Alkyl–Oligo(ethylene oxides).** The PEO–PPO–PEO copolymers are similar (in terms of the PEO head group and the block structure) to the nonionic alkyl oligo(ethylene oxide) surfactants, the phase behavior of which has been widely studied (see refs 26, 39, and 40 and references cited therein). It is appropriate in this respect, to compare the self-assembly features of these two groups of amphiphiles. The alkyl-oligoethylenoxide surfactants form aggregates with curvature toward oil at lower temperatures, while at higher temperatures curvature toward water is favored.[26,29,39,40] In binary systems with water, this property is manifested by the formation of dilute lamellar and $L_3$ ("sponge") phases at higher temperatures in addition to micellar and the usual liquid crystalline phases at lower temperatures.[29] In ternary systems with oil, water-rich microemulsions are formed at lower temperatures, oil-rich microemulsions at higher temperatures, and balanced, bicontinuous microemulsions at intermediate temperatures. The ternary systems also contain water-rich and oil-rich $L_3$ phases and various liquid crystalline phases simultaneously rich in water and oil.[26]

Despite the rich phase behavior, we did not observe balanced bicontinuous microemulsions in the L64–water–xylene system studied here. The alkyl-oligoethylenoxide surfactants have a preferred (spontaneous) curvature, while it appears that in the PEO–PPO–PEO system the curvature of the copolymer film is dictated by the water/oil ratio. However, different oil, temperature, or copolymer PPO–PEO composition may lead to bicontinuous microemulsion topology (further work along these lines is currently in progress in our laboratory). We note that an $L_3$ phase with a narrow temperature stability range has been recently observed[41] in aqueous solutions of $(EO)_6(PO)_{36}(EO)_6$ at ~50 °C. The effect of temperature on the phase behavior has not been considered here. We anticipate that temperature in the PEO–PPO–PEO systems will not have the same effect in the preferred curvature as in the alkyl-oligoethylenoxide systems. In the latter case only the PEO "head group" is affected, while in the former both PEO and PPO blocks are influenced by temperature.[3,6]

**The L64–Water–*o*-Xylene System.** Finally, we turn to the related ternary system L64–water–*o*-xylene, studied recently in a number of papers by Chu and coworkers.[12–15,42,43] Since the solvent properties of *o*-xylene and *p*-xylene are essentially identical, we expect the two systems to behave quantitatively the same. While we have not investigated the phase diagram with *o*-xylene in detail, a number of samples in the *o*-xylene system were prepared, and when compared with the same composition in the *p*-xylene system, the same sequence of phases was observed.

In a recent paper, Wu et al.[15] studied L64–water–*o*-xylene samples prepared with three different initial L64 concentrations in *o*-xylene ($C$ = 0.553, 0.594, and

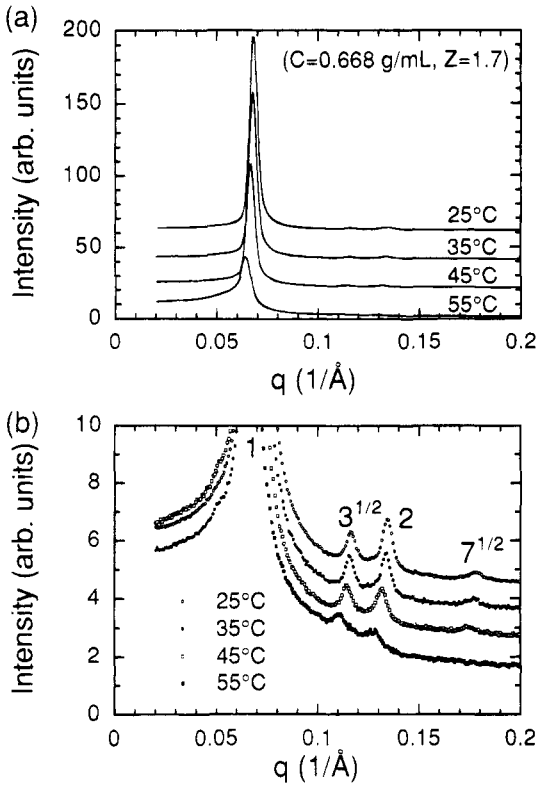


**Figure 8.** (a) Slit-smeared SAXS spectrum obtained from the liquid crystalline phase, previously identified by Wu et al.[14] as lamellar, but shown here to be reverse hexagonal. The L64–$H_2O$–*o*-xylene weight composition is 56.8:15.5:27.7; spectra at 25, 35, 45, and 55 °C are presented. The scattering curves are also shown on an expanded intensity scale (b) to expose the higher order $3^{1/2}$, 2, and $7^{1/2}$ Bragg peaks. The SAXS spectra in both (a) and (b) are drawn on the same scale but are offset vertically for clarity.

0.668 g/mL, respectively) and four different water-to-EO molar ratios, $Z$ ($Z$ = 0.9, 1.3, 1.7, and 2.1, respectively). A diffraction peak at $q = 0.06$ Å$^{-1}$, that shifted only slightly when $Z$ or $C$ varied, was observed in small-angle scattering experiments and attributed to a "lamellar" structure. However, according to the phase diagram of the *p*-xylene system presented here, the compositions studied by Wu et al.[15] fall into the reverse hexagonal ($H_2$) and $H_2$–$L_2$ two-phase regions of the phase diagram (see Figure 1). In order to clarify this discrepancy, we attempted to reproduce some of the experiments reported by Wu et al.[15]

Samples were prepared with the following compositions: $C = 0.553$, $Z = 1.7$; $C = 0.594$, $Z = 1.3$; $C = 0.594$, $Z = 1.7$; $C = 0.594$, $Z = 2.1$; and $C = 0.668$, $Z = 1.7$; where $C$ is the polymer concentration given in grams of L64 per milliliter of solution in *o*-xylene and $Z$ is the ratio of water to EO segments; both normal ($^1H_2O$) and heavy ($^2H_2O$) water were used. After equilibration at 25 °C, only the $C = 0.594$, $Z = 2.1$ and the $C = 0.668$, $Z = 1.7$ samples were single phase; these sample exhibited birefringence under polarized light. The rest of the samples were two-phase systems with the upper phase being fluid, transparent, and isotropic, and the lower phase stiff, transparent, and birefringent. SAXS spectra obtained from the liquid crystalline phase with L64–$H_2O$–*o*-xylene weight composition 56.8:15.5:27.7 ($C = 0.668$, $Z = 1.7$) are presented in Figure 8; spectra at 25, 35, 45, and 55 °C are shown. The scattering curves are shown in Figure 8b on an expanded intensity scale in order to expose the higher order $3^{1/2}$, 2, and $7^{1/2}$ Bragg peaks. The structure of this sample was previously identified by Wu et al.[15] as lamellar, but is clearly shown here to be hexagonal (and more specifically, reverse hexagonal based upon its position in the phase diagram). Furthermore, the hexagonal structure persists up to at least 55 °C. SAXS experiments for the $C = 0.594$, $Z = 2.1$ sample in normal water and the $C = 0.594$, $Z = 2.1$ and $C = 0.668$, $Z = 1.7$ samples in heavy water (SAXS spectra not shown here) also exhibited the $3^{1/2}$, 2, and $7^{1/2}$ peaks, characteristic of a hexagonal structure.[25] We also note that the position of the main SAXS peak (the (10)-reflection) in our experiments is in very good agreement with the $q$ value reported in ref 15. The two-phase samples mentioned above can be attributed to the $H_2$–$L_2$ coexistence region.

Apparently, Wu et al. were not able to observe any higher order reflections that would unequivocally characterize the type of the liquid crystalline structure. We resolved four reflections, namely, $1:3^{1/2}:2:7^{1/2}$ (see Figure 8b), in our SAXS measurements and are thus confident of the structure identification as hexagonal. The case of structure misidentification presented above exemplifies the need for a systematic study of the phase behavior in complex systems (such as the one studied here), as well as the utilization of an array of techniques (e.g., inspection under polarized light, $^2H$ NMR, SAXS) in order to properly characterize the number of phases and the types of the various structures formed.

## CONCLUSIONS

A rich phase behavior with normal hexagonal, lamellar, reverse hexagonal, and bicontinuous cubic liquid crystalline regions, as well as three isotropic liquid phases, was observed at 25 °C in a ternary system of Pluronic L64 (an amphiphilic PEO–PPO–PEO block copolymer), water, and *p*-xylene. The dry block copolymer exists at 25 °C as a disordered melt. Segregation (of the PEO and PPO blocks) and structure are induced by adding water, but not *p*-xylene. The aqueous copolymer solutions have the capability of solubilizing *p*-xylene at most up to ~4% by weight, a rather low uptake which reflects the inability of the L64 micelles to swell. Pluronic L64 is miscible with *p*-xylene in all proportions and forms micelles with a hydrated PEO core and a PPO corona in the presence of water; ~2 water molecules/EO segment can be solubilized in *p*-xylene. A normal hexagonal phase ($H_1$), similar to the micellar $L_1$ phase in terms of xylene solubilization, supersedes $L_1$. A lamellar phase ($L_\alpha$) extends well into the ternary phase diagram and can swell with up to 20 wt % *p*-xylene. A reverse hexagonal phase ($H_2$) is formed between the $L_\alpha$ and $L_2$ phases, extending from 43 to 78 wt % polymer and having ~15–20% water content. A cubic phase is formed between the $L_\alpha$ and $H_2$ regions at high (~75%) polymer concentrations; this phase has been identified as reverse bicontinuous (crystallographic space group *Ia*3*d*). Finally, a very small liquid region present between the normal hexagonal and lamellar phases on the binary water–polymer axis is identified as a melted analogue of a bicontinuous cubic phase.

For L64 concentrations between 50 and 80 wt %, a sequence of liquid crystalline phases (hexagonal, lamellar, reverse cubic, reverse hexagonal) is observed when the water-to-oil ratio is varied, similarly to the sequence of structure attained by dry block copolymers when their block composition is varied. The volume fraction of the apolar components (i.e., PPO and oil) is identified as the major parameter that governs the phase behavior of the PEO–PPO–PEO/water/oil system.

Additional experiments on the related ternary system formulated with *o*-xylene (instead of *p*-xylene) indicate that the phase behavior is insensitive to the choice of the xylene isomer. In particular, we have shown that a reverse hexagonal phase in the *o*-xylene system appears in the same region of the phase diagram as in the *p*-xylene system.

**Acknowledgment.** P.A. is the recipient of a postdoctoral fellowship from the Swedish Natural Science Research Council (NFR). The acquisition of the NMR instruments was partly supported from the Kjell and Märta Beijers Foundation and the Swedish Council for Planning and Coordination of Research (FRN), while the purchase of the SAXS apparatus was funded by FRN. We thank Dr. Ali Khan for helpful discussions.

## References and Notes

(1) Schmolka, I. R. In *Nonionic Surfactants*; Schick, M. J., Ed.; Marcel Dekker: New York, 1967; Chapter 10.
(2) Schmolka, I. R. *J. Am. Oil Chem. Soc.* **1977**, *54*, 110.
(3) Alexandridis, P.; Holzwarth, J. F.; Hatton T. A. *Macromolecules* **1994**, *27*, 2414.
(4) Malmsten, M.; Lindman, B. *Macromolecules* **1992**, *25*, 5440.
(5) Almgren, M.; Brown, W.; Hvidt, S. *Colloid Polym. Sci.* **1995**, *273*, 2.
(6) Alexandridis, P.; Hatton, T. A. *Colloids Surf. A: Physicochem. Eng. Aspects* **1995**, *96*, 1.
(7) Malmsten, M.; Lindman, B. *Macromolecules* **1993**, *26*, 2905.
(8) Wanka, G.; Hoffmann, H.; Ulbricht, W. *Macromolecules* **1994**, *27*, 4145.
(9) Zhang, K.; Khan, A. *Macromolecules* **1995**, *28*, 3807.
(10) Alexandridis, P.; Zhou, D.; Khan, A., submitted for publication.
(11) Hurter, P. N.; Alexandridis, P.; Hatton, T. A. In *Solubilization in Surfactant Aggregates*; Christian, S. D., Scamehorn, J. F., Eds.; Marcel Dekker: New York, 1995; Chapter 6.
(12) Wu, G.; Zhou, Z.; Chu, B. *Macromolecules* **1993**, *26*, 2117.
(13) Wu, G.; Zhou, Z.; Chu, B. *J. Polym. Sci., Polym. Phys. Ed.* **1993**, *31*, 2035.
(14) Wu, G.; Chu, B.; Schneider, D. K. *J. Phys. Chem.* **1994**, *98*, 12018.
(15) Wu, G.; Ying, Q.; Chu, B. *Macromolecules* **1994**, *27*, 5758.
(16) Rosevear, F. B. *J. Am. Oil Chem. Soc.* **1954**, *31*, 628.
(17) Halle, B.; Wennerström, H. *J. Chem. Phys.* **1981**, *75*, 1928.
(18) Lindman, B.; Olsson, U.; Söderman, O. In *Dynamics of Solutions and Fluid Mixtures by NMR*; Delpuech, J.-J., Ed.; John Wiley & Sons: London, 1995; Chapter 8.
(19) Alexandridis, P.; Nivaggioli, T.; Hatton, T. A. *Langmuir* **1995**, *11*, 1468.
(20) Gadelle, F.; Koros, W. J.; Schechter, R. S. *Macromolecules* **1995**, *28*, 4883.
(21) Khan, A.; Fontell, K.; Lindblom, G.; Lindman, B. *J. Phys. Chem.* **1982**, *86*, 4266.
(22) Nivaggioli, T.; Alexandridis, P.; Hatton, T. A.; Yekta, A.; Winnik, M. A. *Langmuir* **1995**, *11*, 730.
(23) Friberg, S.; Jansson, P. O.; Cederberg, E. *J. Colloid Interface Sci.* **1976**, *55*, 614.
(24) Walderhaug, H.; Hansen, F. K.; Abrahmsen, S.; Persson, K.; Stilbs, P. *J. Phys. Chem.* **1993**, *97*, 8336.
(25) *International Tables for Crystallography*; D. Reidel Publishing Company: Dordrecht, The Netherlands, 1983; Vol A.
(26) Olsson, U.; Würz, U.; Strey, R. *J. Phys. Chem.* **1993**, *97*, 4535.
(27) Fontell, K. *Colloid Polym. Sci.* **1990**, *268*, 264.
(28) Scriven, L. E. *Nature* **1976**, *263*, 123.
(29) Anderson, D.; Wennerström, H.; Olsson, U. *J. Phys. Chem.* **1989**, *93*, 4243.
(30) Mariani, P.; Luzzati, V.; Delacroix, H. *J. Mol. Biol.* **1988**, *204*, 165.
(31) Clerc, M.; Dubois-Violette, E. *J. Phys. II Fr.* **1994**, *4*, 275.
(32) Hyde, S. T. *J. Phys. Chem.* **1989**, *93*, 1458.
(33) Anderson, D. M.; Davis, H. T.; Scriven, L. E.; Nitsche, J. C. C. *Adv. Chem. Phys.* **1990**, *77*, 337.
(34) Anderson, D. M.; Ström. P. *ACS Symp. Ser.* **1989**, *No. 384*, 204.
(35) Alexandridis, P.; Athanassiou, V.; Fukuda, S.; Hatton, T. A. *Langmuir* **1994**, *10*, 2604.
(36) Wong, T. C.; Ikeda, K.; Meguro, K.; Söderman, O.; Olsson, U.; Lindman, B. *J. Phys. Chem.* **1989**, *93*, 4861.
(37) Forrest, B. J.; de Carvalho, L. H.; Reeves, L. W. *J. Am. Chem. Soc.* **1981**, *103*, 245.
(38) Bates, F. S. *Science* **1991**, *251*, 898.
(39) Olsson, U.; Wennerström, H. *Adv. Colloid Interface Sci.* **1994**, *49*, 113.
(40) Strey, R. *Colloid Polym. Sci.* **1994**, *272*, 1005.
(41) Hecht, E.; Mortensen, K.; Hoffmann, H. *Macromolecules* **1995**, *28*, 5465.
(42) Chu, B.; Wu, G. *Macromol. Symp.* **1995**, *90*, 251.
(43) Chu, B. *Langmuir* **1995**, *11*, 414.

MA950713F